Received: 24 April 2023 | Revised: 11 July 2023 | Accepted: 6 August 2023

DOI: 10.1002/bit.28530

ARTICLE

BIOTECHNOLOGY AND BIOENGINEERING WILEY

# Characterization of a quail suspension cell line for production of a fusogenic oncolytic virus

Sven Göbel[1] | Karim E. Jaén[1,2] | Rita P. Fernandes[3] | Manfred Reiter[4] | Jennifer Altomonte[2] | Udo Reichl[1,5] | Yvonne Genzel[1]

[1]Bioprocess Engineering, Max Planck Institute for Dynamics of Complex Technical Systems, Magdeburg, Germany

[2]Department of Internal Medicine II, Klinikum Rechts der Isar, Technische Universität München, Munich, Germany

[3]Instituto de Biologia Experimental e Tecnológica (iBET), Oeiras, Portugal

[4]Nuvonis Technologies GmbH, Vienna, Austria

[5]Chair for Bioprocess Engineering, Otto-von-Guericke-University Magdeburg, Magdeburg, Germany

**Correspondence**

Yvonne Genzel, Bioprocess Engineering, Max Planck Institute for Dynamics of Complex Technical Systems, Sandtorstr. 1, 39106 Magdeburg, Germany.
Email: genzel@mpi-magdeburg.mpg.de

**Funding information**

Federal Ministry for Economic Affairs and Energy, Grant/Award Number: #03EFOBY215

## Abstract

The development of efficient processes for the production of oncolytic viruses (OV) plays a crucial role regarding the clinical success of virotherapy. Although many different OV platforms are currently under investigation, manufacturing of such viruses still mainly relies on static adherent cell cultures, which bear many challenges, particularly for fusogenic OVs. Availability of GMP-compliant continuous cell lines is limited, further complicating the development of commercially viable products. BHK21, AGE1. CR and HEK293 cells were previously identified as possible cell substrates for the recombinant vesicular stomatitis virus (rVSV)-based fusogenic OV, rVSV-NDV. Now, another promising cell substrate was identified, the CCX.E10 cell line, developed by Nuvonis Technologies. This suspension cell line is considered non-GMO as no foreign genes or viral sequences were used for its development. The CCX.E10 cells were thus thoroughly investigated as a potential candidate for OV production. Cell growth in the chemically defined medium in suspension resulted in concentrations up to $8.9 \times 10^6$ cells/mL with a doubling time of 26.6 h in batch mode. Cultivation and production of rVSV-NDV, was demonstrated successfully for various cultivation systems (ambr15, shake flask, stirred tank reactor, and orbitally shaken bioreactor) at vessel scales ranging from 15 mL to 10 L. High infectious virus titers of up to $4.2 \times 10^8$ $TCID_{50}$/mL were reached in orbitally shaken bioreactors and stirred tank reactors in batch mode, respectively. Our results suggest that CCX.E10 cells are a very promising option for industrial production of OVs, particularly for fusogenic VSV-based constructs.

**KEYWORDS**

ambr15, avian suspension cells, cell culture-based production, fusogenic oncolytic virus, upstream processing

**Abbreviations:** CCX.E10, QOR2/2E11 cells; CSVY, cell-specific virus yield; GMP, good manufacturing practice; hpi, hours postinfection; MOI, multiplicity of infection; NDV, Newcastle disease virus; OSB, orbitally shaken bioreactor; OTR, oxygen transfer rate; OV, oncolytic virus; $q_{glc}$, cell-specific glucose uptake rate; $q_{lac}$, cell-specific lactate production rate; $q_{NH4}$, cell-specific ammonium production rate; rVSV-NDV, recombinant hybrid virus: VSV backbone and surface glycoproteins of NDV used in this study; SCGM, supplemented Freestyle293 expression medium; STR, stirred tank bioreactor; $TCID_{50}$, 50% tissue culture infectious dose; TOI, time of infection; VCC, viable cell concentration; VSV, vesicular stomatitis virus; VVP, volumetric virus productivity; vw, working volume; μ, cell-specific growth rate.

## 1 | INTRODUCTION

Oncolytic virotherapy describes the use of oncolytic viruses (OVs) to selectively infect and kill cancerous cells as a treatment against various types of cancer. By utilizing the natural propensity of OVs to exploit various defects in cellular antiviral pathways often present in cancer cells, a direct destruction through oncolysis without harming surrounding healthy cells can be achieved, with a secondary therapeutic initiation of systemic antitumor immune responses (Flint, 2020). Modification of OVs through genetic engineering, for example, expression of optimized endogenous or heterologous fusion glycoproteins can further improve their efficacy. rVSV-NDV, a recombinant vesicular stomatitis virus (VSV) backbone with fusogenic mutant glycoproteins of Newcastle disease virus (NDV) demonstrated promising preclinical data in both single and combination therapy in various cancer models (Abdullahi et al., 2018; Krabbe et al., 2021).

The majority of OVs currently under development and in clinical testing are being produced in static adherent cell cultures (Ungerechts et al., 2016). Talimogene laherparepvec, so far the only approved OV in the market, is manufactured in adherent Vero cells using roller bottles, where the collected harvest is pooled and purified in several steps comprising endonuclease digestion, clarification by filtration, ultrafiltration/diafiltration, two chromatography steps (ion exchange + size exclusion), and a final sterile filtration (EMA, 2015). Specific properties of fusogenic OVs, for example, the formation of large multinucleated syncytia that die rapidly after induction, present unique challenges for large-scale clinical-grade manufacturing. Despite screening of several adherent cell lines, relatively low virus yields were achieved for rVSV-NDV, so far (Göbel et al., 2022). Ideally, producer cell lines should: i) show sufficient susceptibility to the respective OV, ii) demonstrate robust growth in suspension culture with doubling times <30 h, iii) allow to generate high virus titers in chemically defined media, and iv) meet regulatory requirements, for example, documented origin, full characterization, stability, and absence of tumorigenicity. Using a suspension HEK293 producer cell line fulfilling most of these requirements, Pelareorep, a non-fusogenic oncolytic reovirus, is produced in stirred-tank bioreactors followed by a multistep purification train and is currently under investigation in clinical phase III trials for the treatment of metastatic breast cancer (Ungerechts et al., 2016).

So far, there are only a few continuous cell lines available for clinical-grade OV manufacturing. These include mainly Vero cells (herpesvirus, measles virus, and vaccinia virus), A549 cells (adenovirus), HeLa cells (vaccinia virus), HEK293 cells (adenovirus, reovirus), and some proprietary cell lines (e.g., EB66, PER.C6, and CAP) (Ungerechts et al., 2016). Other continuous suspension cell lines, such as BHK-21, AGE1.CR, MDCK, and HEK293SF cells, have been evaluated for efficient production of fusogenic rVSV-NDV (Göbel, 2022, 2023). The highest reported rVSV-NDV yields were obtained in BHK-21 suspension cells with titers up to $5 \times 10^8$ $TCID_{50}$/mL in optimized batch processes in stirred tanks and $2 \times 10^9$ $TCID_{50}$/mL in perfusion cultures infected at high cell density (Göbel, 2023). First studies performed with the avian cell line AGE1.CR, which is fully characterized and GMP-compliant, resulted in relatively low virus yields. Although therapeutic indications of OVs may allow a different risk-benefits analysis compared with traditional viral vaccines, and fewer constraints regarding the use of cell lines known to be tumorigenic or possessing abnormal karyology (ICH, 1998; Jordan & Sandig, 2014), cell substrates demonstrating a good safety profile should be preferred.

In this study, we investigated an immortalized continuous suspension cell line derived from quail cells CCX.E10 (Nuvonis Technologies GmbH). CCX.E10 cells were extensively characterized by Nuvonis Technologies. They fulfill all critical regulatory requirements, are grown in chemically defined medium, and are qualified as source material for Good Manufacturing Practice (GMP)-compliant production (Kraus et al., 2011). Therefore, these cells represent a valuable alternative for high-yield production of VSV-NDV without the regulatory risks associated with BHK-21. For the first time, a fully scalable, production process in quail suspension cells for the fusogenic rVSV-NDV OV is described. Both upstream and downstream processing aspects were considered to assess the efficiency of the established production train. High rVSV-NDV yields were obtained in batch mode in various production systems at different vessel scales (15 mL–10 L) with maximum titers up to $4.2 \times 10^8 TCID_{50}$/mL.

## 2 | MATERIALS AND METHODS

### 2.1 | Cell culture, media, and viral seed stock

SCGM suspension cell growth medium was used for CCX.E10 cells. SCGM is based on the commercially available chemically defined Freestyle™293 Expression medium (Gibco), but is supplemented with growth factors.

Cells were cultivated in baffled 125 mL shake flasks with vent caps (Corning) with a working volume (vw) of 50 mL. A Multitron orbitally shaken incubator (Infors AG) with 50 mm shaking diameter was used to incubate cells at 185 rpm, 37°C, and 5% $CO_2$. Cells were inoculated at a cell concentration of $0.8 \times 10^6$ cells/mL and passaged twice per week.

For all infections, a CCX.E10 cell-derived virus seed (rVSV-NDV) concentrated by ultracentrifugation, followed by purification on sucrose gradients ($1.05 \times 10^8$ $TCID_{50}$/mL), was used in this study.

### 2.2 | Batch cultivations in orbitally shaken bioreactors

For infection studies in shake flasks, CCX.E10 cells were inoculated at $0.4 \times 10^6$ cells/mL and cultivated for 96 h to reach about $4.0 \times 10^6$ cells/mL. At time of infection (TOI), the viable cell concentration (VCC) was adjusted to $2 \times 10^6$ cells/mL by either diluting the vw two-fold with fresh medium or by centrifugation of the appropriate volume at 300*g* for 5 min and re-suspending the cells in fresh

medium. Cells were subsequently infected at a multiplicity of infection (MOI) of 1E-4 with rVSV-NDV.

Cultivation in the SB10-X orbital shaken bioreactor (OSB) (Adolf Kühner AG) was carried out with a 12 L single-use standard bag. CCX.E10 cells were inoculated at $0.8 \times 10^6$ cells/mL with 3 L initial vw at 37°C with a shaking frequency of 100 rpm (50 mm shaking diameter). Aeration was carried out through headspace gassing at a rate of 300 mL/min with air. Partial pressure of dissolved oxygen (DO) and pH values were controlled at 80% and 7.3, respectively, by automatic adjustment of the gas composition in the output flow. At TOI, the bioreactor vw was increased from 3 L to 6 L with fresh medium containing virus. CCX.E10 cells were infected with an MOI of 1E-4 and temperature was decreased to 34°C.

## 2.3 | Batch cultivations in STR and ambr15

Bioreactor cultivations in 1 L DASGIP bioreactor systems (Eppendorf AG) were used with 350 mL initial vw. Bioreactors were inoculated from shake flask pre-cultures at a VCC of $0.8 \times 10^6$ cells/mL. Cells were agitated with a pitched blade impeller (50 mm diameter) at 80–180 rpm (upflow) with aeration by a submerged L-drilled hole sparger. pH value was controlled at 7.2 by sparging $CO_2$. Oxygen and nitrogen flow rates were controlled between 3–9 L/h to maintain a DO level equal or above 50%. Temperature was set at 37°C for the growth phase and 34°C for the infection phase. At TOI, cells were infected at an MOI of 1E-4 by addition of an equal vw of pre-warmed fresh medium containing rVSV-NDV (350 mL).

The bioreactor cultivation in a 3 L DASGIP bioreactor system (Eppendorf AG) was started with 1300 mL initial vw. For agitation, two pitched blade impellers (50 mm diameter) at 180 rpm (upflow) with aeration by a submerged L-drilled hole sparger were used. To maintain a DO level equal or above 50%, oxygen and nitrogen flow rates were controlled between 9 and 12 L/h. Inoculation and process parameters were identical to the previously described 1 L system.

Cultivations in the ambr15™ unit (kindly provided by Sartorius AG) were carried out with a vw of 15 mL. The reactor volume was kept above 10 mL throughout the cultivation for all vessels. DO was controlled at 50% by oxygen enrichment through a pipe sparger and pH was controlled by $CO_2$ enrichment or addition of 7.5% $NaHCO_3$. Off-set adjustments of pH were carried out daily by off-line measurement with an additional pH7110 potentiometer (Inolab). The effects of pH adjustments to 7.0, 7.2, or 7.4 during cell growth and virus production were evaluated. Agitation speed of the integrated pitched blade impeller (diameter = 11.4 mm) was scaled down based on tip-speed of the 1 L STR experiment and set to 800 rpm. Individual ambr vessels were sampled daily to measure VCC, offline-pH, and virus titer.

## 2.4 | Analytics

An automated cell counter (ViCell; Coulter Beckman) was used to determine VCC and viability. Off-line pH was measured in a pH7110 potentiometer (Inolab), and lactate, ammonium, glutamine, glutamate, and glucose were determined with a Cedex Bio Analyzer (Roche). To allow easier handling, virus-containing samples were heat-inactivated at 80°C for 3 min before metabolite measurements. For titration of rVSV-NDV, the previously described $TCID_{50}$ assay (Göbel et al., 2022) was performed using adherent AGE1.CR.pIX cells (kindly provided by ProBioGen). The cell-specific virus yields (CSVY) was calculated as previously described by Gränicher et al. (2020). taking into account only the error of the $TCID_{50}$ assay (−50%/ + 100% on a linear scale). Total protein was assessed with Pierce™ BCA assay kit (ThermoFisher) and total DNA was quantified with Quant-iT™ PicoGreen dsDNA assay kit (ThermoFisher) used according to the manufacturer's instructions. Cell-specific substrate consumption rates ($q_s$) were determined as described by Gränicher et al. (2020).

$$q_s = \frac{\mu}{Y_{x/s}} \tag{1}$$

$$Y_{x/s} = \frac{x(t_{n+1}) - x(t_n)}{c_s(t_n) - c_s(t_{n+1})}, \tag{2}$$

where $x$ is the VCC, $t$ is the cultivation time, $n$ is the sampling time point, and $c_s$ is the cell culture compound concentration.

# 3 | RESULTS AND DISCUSSION

Addressing key parameters in both the cell growth and virus production phase is critical for the evaluation of a cell substrate for the production of fusogenic oncolytic viruses. Therefore, in the first step, the transfer to orbitally shaken systems from stirred spinner flask systems was investigated. Here, baseline cell growth over multiple passages and metabolism of the CCX.E10 cell line was evaluated in the absence of virus infection. Subsequently, rVSV-NDV production was characterized and optimized in batch mode in various production systems at different scales (15 mL–6 L).

## 3.1 | Evaluation of cell growth after transfer to orbitally shaken systems

Until now, CCX.E10 cells were sub-cultured in spinner flasks, reaching only moderate viable cell concentrations (up to $2.0–3.0 \times 10^6$ cells/mL) after multiple days of growth (Reiter et al., 2014). A direct transfer to an orbitally shaken environment, by thawing the cells in unbaffled shake flasks and splitting to baffled shake flasks after passage 2, resulted in a lag phase of 7 days without a negative impact on cell viability (Figure 1a). As thawing is a harsh and stressful procedure for most animal cells, delays in cell growth are common (González Hernández, 2007). Although shear rates are lower in shake flasks compared to stirred tanks (Giese et al., 2014), the direct transfer to the new orbitally shaken environment was expected to cause a lag phase. However, after Day 10, robust cell growth up to $4.0–6.0 \times 10^6$ cells/mL, with doubling times of around

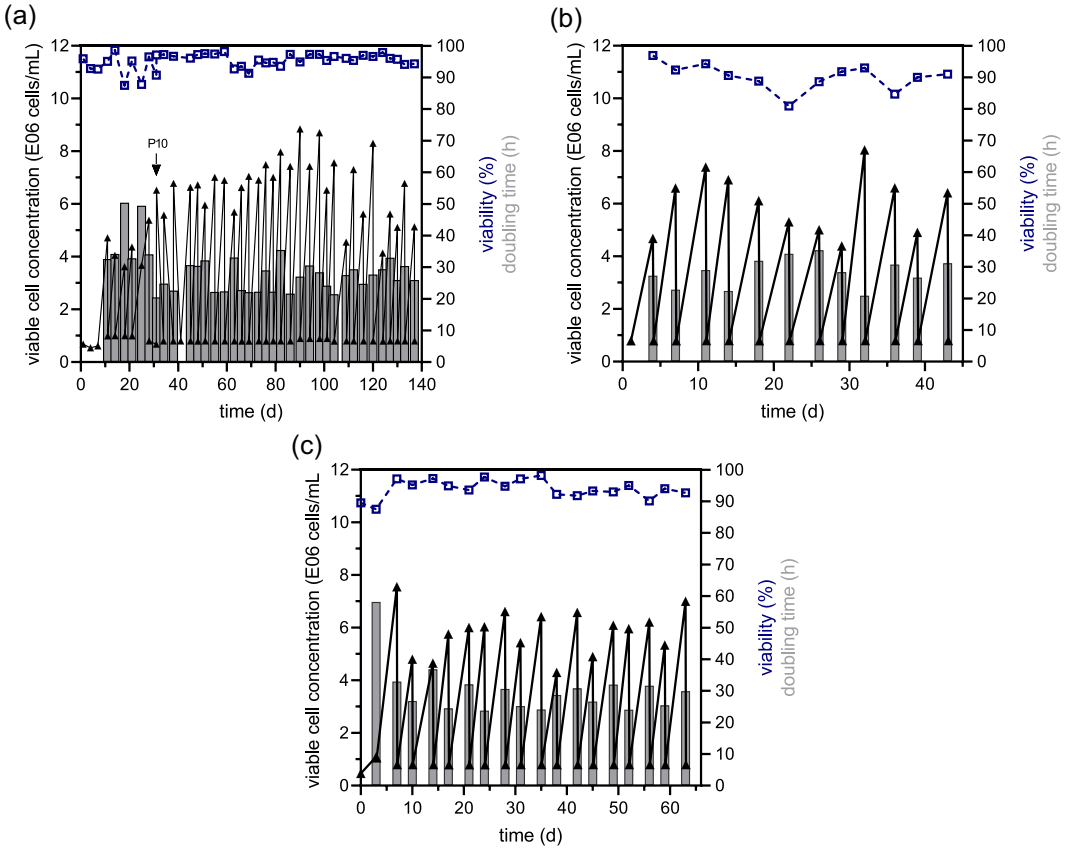


**FIGURE 1** Serial passaging of CCX.E10 cells and adaptation to growth in an orbitally shaken system. CCX.E10 cells were first thawed in 125 mL unbaffled shake flasks and subsequently transferred to 125 mL baffled shake flasks after passage 2 (all wv: 50 mL, 50 mm shaking diameter, 185 rpm, 37°C, 5% $CO_2$). Here, CCX.E10 cells were cultivated over 40 passages, and average doubling time (gray bars), viable cell concentration (black squares), and viability (blue empty squares) were recorded. (a) Cultivation in SCGM medium. (b) Cultivation starting from P10 in SCGM medium without putrescine dihydrochloride. (c) Cultivation of adapted cell bank generated at P10 in SCGM medium. CCX.E10, QOR2/2E11 cells; SCGM, supplemented Freestyle293 expression medium.

30–50 h was achieved. By Day 30, the average doubling time decreased to 25–30 h and was maintained until end of cultivation (140 d). At Day 30 (passage 10), cells were considered to be fully adapted to growth in the orbital shaker, and a cell bank was established for all further experiments. Interestingly, even higher maximum cell concentrations of up to $8.8 \times 10^6$ cells/mL with high viabilities (above 97%) were reached between Days 60 and 120 (Figure 1a). Over the entire cultivation period, CCX.E10 cells had an average doubling time of 29 h and an average cell diameter of 15.2 µm. Putrescine dihydrochloride is a common component in cell culture medium (e.g., Dulbecco's Modified Eagle Medium F12) and has an established role on regulation of division, differentiation and maturation of cells, DNA and RNA synthesis as well as apoptosis (Hesterberg et al., 2018; Zdrojewicz & Lachowski, 2014). However, due to the acute toxicity (category 3–4) for humans, subpassaging without this compound was carried out. Omission of putrescine dihydrochloride in a sub-culture of passage 10, had a negative impact on the average doubling time (29 h compared with 26.6 h) compared to the fully supplemented medium. Moreover, a decrease in maximum viable cell concentrations as well as a reduced viability (below 90%) was observed from passage 2–12 (Figure 1b). Although maximum viable cell concentration recovered after passage 12, cell viability remained low around 90%. After thawing adapted cells (P10) in shake flasks, no lag phase was observed and cells grew up to $6.0 \times 10^6$ cells/mL with high viabilities in further passages (Figure 1c). As demonstrated for CHO cells, once cells have physiologically adapted to a new environment, here an orbitally shaken system, their growth performance remained stable as long as cultivation parameters were kept (Wurm & Wurm, 2021).

Fully adapted CCX.E10 cells were able to grow to cell concentrations above $8.5 \times 10^6$ cells/mL with low doubling times of 26.6 ± 2.6 h in batch mode (Figure 2a, Table 1). Viability remained above 96% over the cell growth phase and only decreased from 96 h onwards after the maximum cell concentration was reached and after glucose was depleted (Figure 2a,b). The depletion of critical nutrients (e.g., glucose) is well known to limit cell growth and to cause a decrease in cell viability (Tsao et al., 2005). Accumulation of secondary by-products of metabolism such as lactate (above 20 mM) and ammonium (2–3 mM) have also been shown to negatively impact cell growth and virus production (Schneider, 1996). However, these limits were not exceeded during the exponential growth phase (Figure 2b).

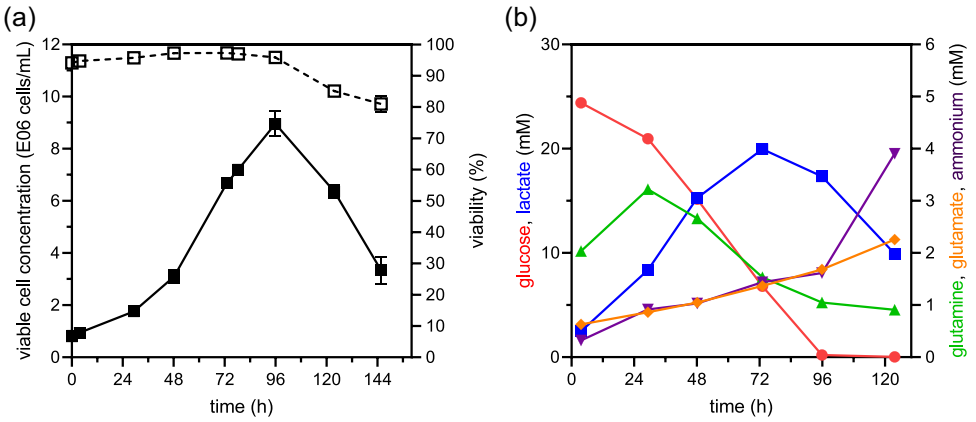


**FIGURE 2** Growth and metabolism of CCX.E10 cells in SCGM medium in shake flasks. CCX.E10 cells were inoculated at $0.8 \times 10^6$ cells/mL and cultivated in baffled 125 mL shake flasks. (a) viable cell concentration (full squares) and viability (empty squares), (b) glucose (red circles), lactate (blue squares), glutamine (green triangles), glutamate (orange triangles), and ammonium (purple triangles) concentrations. Values are reported as the mean ± SD of biological replicates ($n = 3$). CCX.E10, QOR2/2E11 cells; SCGM, supplemented Freestyle293 expression medium; SD, standard deviation.

**TABLE 1** Calculated parameters for CCX.E10 cells cultivated in batch mode in shake flasks.

| | Cultivation time range (h) | Shake flask ($n = 3$) |
|---|---|---|
| Cell-specific growth rate (1/h) | 0–96 | 0.026 ± 0.003 |
| Doubling time (h) | 0–96 | 26.6 ± 2.6 |
| Cell diameter | 0–96 | 15.7 ± 0.12 |
| qGlc ($10^{-11}$*mmol/(cell*h)) | 0–96 | −7.9 ± 0.6 |
| qLac ($10^{-11}$*mmol/(cell*h)) | 0–72 | 8.6 ± 0.9 |
| $qNH_{4+}$ ($10^{-11}$*mmol/(cell*h)) | 0–123 | 0.4 ± 0.04 |

*Note*: Values are reported as the mean±SD of biological replicates ($n = 3$). Abbreviations: CCX.E10, QOR2/2E11 cells; max., maximum (see Equation 1); qGlc, cell-specific glucose consumption rate; qLac, cell-specific lactate release rate; qNH4+, cell-specific ammonium release rate; SD, standard deviation.

Similar to mammalian cells, such as HEK293 cells (Petiot et al., 2015), MDCK cells (Bissinger et al., 2019) and PBG.PK2.1 cells (Gränicher et al., 2019), CCX.E10 cells shifted their metabolism from lactate production towards lactate consumption in the middle of the cultivation period once glucose level was less than 10 mM (Figure 2b). As Freestyle medium contains the supplement GlutaMAX™, the measured glutamine concentrations do not accurately represent the freely available glutamine in the culture medium. However, accumulation of glutamate over the cultivation time suggested an active glutamine metabolism (Figure 2b) (Newsholme et al., 2003). The cell-specific glucose uptake rate $q_{glc}$ of −7.9±0.6×$10^{-11}$mmol/(cell*h) (Table 1) and the lactate yield based on glucose consumption $Y_{lac/glc}$ of 0.9 were in the range observed for other avian cell lines, such as AGE1.CR.pIX, with $q_{glc}$ varying between 5 and $7.5 \times 10^{-11}$ mmol/(cell*h) and $Y_{lac/glc}$ of 0.8–1 mmol/cell (Coronel et al., 2020).

The achieved doubling time and maximum cell concentration are not only comparable to other avian suspension cell lines, such as AGE1.CR cells (25 h; $8.7 \times 10^6$ cells/mL (Coronel et al., 2019; Genzel et al., 2014a), AGE1.CR.pIX cells (27.5 h; $13.0 \times 10^6$ cells/mL (Coronel et al., 2019; Lohr, 2014; Lohr, Hädicke, et al., 2014), EB66 cells (19–23 h; $14.0 \times 10^6$ cells/mL; Nikolay et al., 2018), and DuckCelt®-T17 (29 h; $6.5 \times 10^6$ cells/mL; Petiot et al., 2018) but also to MDCK suspension cells (20 h; $10.0 \times 10^6$ cells/mL; Bissinger et al., 2019), BHK-21 cells (25 h; Göbel, 2023), and HEK293 suspension cells (33 h; $4.0–5.0 \times 10^6$ cells/mL; Abaandou et al., 2021) cultivated in batch mode.

## 3.2 | Virus propagation in orbitally shaken systems

MOI effects have been thoroughly investigated for a variety of virus-host cell systems. Particularly for rVSV-NDV, the optimal MOI seems to be highly cell-line dependent (Göbel et al., 2022). Consequently, evaluations of MOI ranging from 1E-2–1E-5 were performed with rVSV-NDV for the CCX.E10 cells. Although similar maximum infectious virus titers were reached for all MOIs, 1E-4 was identified as optimal as the highest virus titers were reached (data not shown). Subsequently, the effect of a medium exchange at TOI was analyzed and compared with a two-fold dilution with fresh medium (at TOI). Growth parameters after infection, as well as virus replication dynamics were very similar for both conditions (Figure 3a,b). Maximum titers of $5.0 \times 10^8 \pm 2.2 \times 10^8$ $TCID_{50}$/mL and $3.2 \times 10^8$ $TCID_{50}$/mL and CSVYs of 110 ± 43 and 83 ± 9 $TCID_{50}$/cell were reached for the two-fold dilution and complete medium exchange, respectively. This was surprising as previous studies using avian AGE1.CR cultures for production of rVSV-NDV showed only moderate virus titers when switching from a complete medium exchange at TOI in shake flask cultures to a two-fold dilution in STRs (Göbel, 2023). Moreover, it has been reported that providing an optimal metabolic state with a sufficient supply of substrates plus removal of inhibiting molecules by a complete media exchange, led to

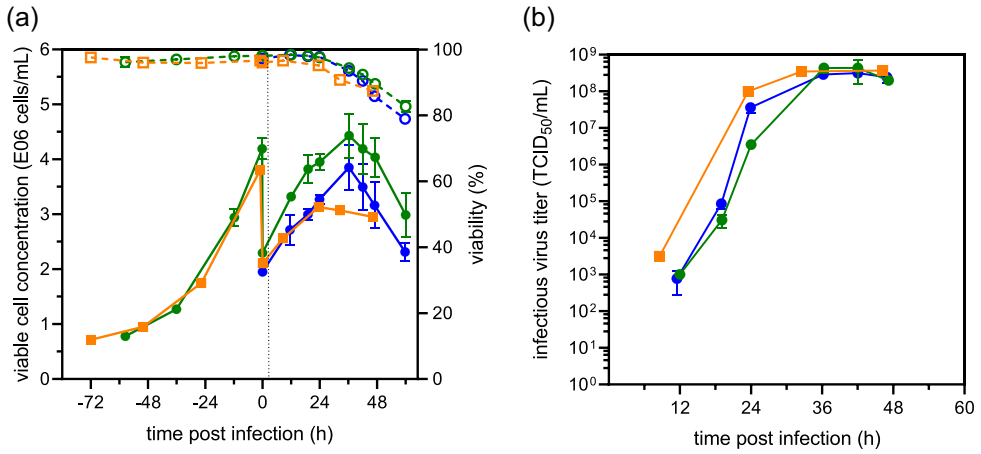


**FIGURE 3** rVSV-NDV production in CCX.E10 cells in a shaker flask compared to an orbitally shaken system. Cells were grown in 125 mL baffled shake flasks (circles) or in the SB10-X bioreactor (squares) and infected at an MOI of 1E-4 at $2 \times 10^6$ cells/mL. To determine the effect of a medium exchange at TOI, the medium was either exchanged completely (blue circles) or diluted two-fold with fresh SCGM medium (green circles). Scale-up to SB10-X bioreactor with two-fold dilution at TOI (orange square). (a) Cell growth (full symbols) and viability (empty symbols); (b) infectious virus titers determined by $TCID_{50}$ assay. Values for shake flasks are reported as the mean±SD of biological replicates ($n = 3$). CCX.E10, QOR2/2E11 cells; MOI, multiplicity of infection; SCGM, supplemented Freestyle293 expression medium; SD, standard deviation; TOI, time of infection.

increased titers for various viruses (Genzel et al., 2014a; Elahi et al., 2019; Vázquez-Ramírez et al., 2018). Most likely, a two-fold dilution with fresh supplemented SCGM medium provided enough essential nutrients necessary for optimal virus replication while also reducing the concentration of inhibiting or toxic by-products from metabolism. Therefore, no reductions of virus titers by metabolic limitations and accumulation of inhibiting molecules were expected for subsequent scale-up experiments in OSBs and STRs. As hypothesized, maximum infectious virus titers achieved following a complete medium exchange were in the same range compared to the previously identified optimal cell substrate, BHK-21, but 0.6-1.0 log higher than for HEK293 and AGE1.CR cells (Göbel et al., 2022).

In a second step, the virus production process was scaled-up from a 125 mL shake flask on an orbital platform to a single-use SB10-X OSB. Both cultures displayed cell viabilities exceeding 95% and a consistent growth with a $\mu$ of 0.024 1/h and a doubling time of 28.8 h during the exponential growth phase. VCC increased until 24–36 h postinfection (hpi), reaching maximum concentrations of $3–4.2 \times 10^6$ cells/mL, after which VCC and viability steadily decreased until the end of the cultivation (Figure 3a). Maximum cell concentrations postinfection were slightly higher in shake flask cultures compared to the SB10-X, most likely due to batch-to-batch variability. Overall maximum infectious virus titers of $3.7–4.2 \times 10^8$ $TCID_{50}$/mL (Figure 3b) and CSVY of 118–121 $TCID_{50}$/cell (Table 2) were achieved at 29–32 hpi, respectively. The $k_La$ for the shake flask for the described culture conditions (37°C, 185 rpm, 50 mL vw) was estimated based on correlations from Schiefelbein et al. (2013). For the SB10-X bioreactor, the $k_La$ was determined for a shaking frequency of 100 rpm and a vw of 6 L, as described by Kühner (AG, 2017). For the described conditions, a $k_La$ of 99 1/h for the baffled shake flask and 15 1/h for the SB10-X should be expected. In addition, oxygen transfer rates (OTRs) for the shake flask and SB10-X were calculated based on correlations from Meier et al. (2016). and (AG, 2017), respectively. Here, OTRs of 11 mmol/(L*h) for the shake flask and 3 mmol/(L*h) for SB10-X were calculated. The $k_La$ and OTR were not maintained throughout the scale up, but kept above 10 1/h and 1 mmol/(L*h) to ensure a sufficient amount of oxygen. On the other hand, mixing times in the shake flask (~3 s (Tan et al., 2011)) and the SB10-X approximately 5 s (AG, 2017)) were kept constant across scales. This underlines the facilitated scale-up (over two orders of magnitude) in orbitally shaken systems with similar geometrical characteristics when mixing and aeration principles are maintained (Klöckner et al., 2014).

## 3.3 | Virus production in STR

As an alternative production system, cells were cultivated in DASGIP bioreactors with 350 mL vw using the previously optimized MOI and medium dilution at TOI. To identify optimal cultivation conditions for both growth and virus production, different agitation speeds (80–180 rpm) were evaluated. Here, cells were cultivated until a VCC of $4.0 \times 10^6$ cells/mL was achieved and diluted two-fold with fresh medium before infection. During cell growth, the lowest $\mu = 0.017$ 1/h, corresponding to a doubling time of 40.8 h was achieved for 80 rpm (Table 2). Low agitation speeds can lead to insufficient mixing, causing localized areas of nutrient depletion and suboptimal conditions for cell growth. Moreover, lower oxygen transfer rates are achieved, potentially resulting in reduced cell growth rates and cell viabilities. However, viability remained constantly above 96% for all conditions (Figure 4a). Compared to shake flask cultivations (Figure 3), slightly higher doubling times but no major differences in cell viability or average cell diameter were detected. Different metabolite profiles were observed for the different stirring speeds: The prolonged growth phase of cells cultivated

**TABLE 2** rVSV-NDV production in CCX.E10 cells considering key parameters for both upstream and downstream processing. Cell growth parameters were determined before infection.

| | SF | SB10-X | STR 1 L 80 rpm | 130 rpm | 180 rpm | STR 3 L 180 rpm | ambr15 |
|---|---|---|---|---|---|---|---|
| Cell-specific growth rate (1/h) | 0.026 | 0.024 | 0.017 | 0.022 | 0.022 | 0.024 | 0.022 |
| Doubling time (h) | 26.6 | 28.9 | 40.7 | 31.5 | 31.5 | 28.9 | 31.5 |
| qGlc ($10^{-11}$*mmol/(cell*h)) | −7.9 | n.d. | −18.8 | −15.8 | −15.9 | −13.5 | n.d. |
| qLac ($10^{-11}$*mmol/(cell*h)) | 8.6 | n.d. | 15.3 | 16.4 | 15.3 | 12.3 | n.d. |
| $qNH_{4+}$ ($10^{-11}$*mmol/(cell*h)) | 0.4 | n.d. | 0.3 | 0.6 | 0.6 | 0.8 | n.d. |
| Total process time (h) | 126 | 118 | 177 | 152 | 142 | 143 | 128 |
| max. VCC p.i. ($10^6$ cells/mL) | 4.4 | 3.1 | 3.7 | 4.2 | 3.4 | 4.2 | 3.6 |
| max. infectious virus titer ($10^8$ $TCID_{50}$/mL) | 5.0 | 3.7 | 0.1 | 1.8 | 3.2 | 4.2 | 1.0-2.0 |
| CSVY ($TCID_{50}$/cell) | 111 | 118 | 3 | 42 | 94 | 100 | 70 |
| VVP ($10^{10}$ virions/L/d) | 10.2 | 7.5 | 0.1 | 2.8 | 5.2 | 7.0 | 2.0 |
| dsDNA impurity level at optimal harvest time point (µg/mL) | n.d. | n.d. | 6.8 | 16.5 | 9.7 | 14.1 | n.d. |
| Protein impurity level at optimal harvest time point (mg/mL) | n.d. | n.d. | 2.3 | 1.8 | 2.5 | 2.0 | n.d. |

*Note*: Optimal harvest time point was defined as time point when the maximum infectious virus titer with lowest impurity level was reached in the supernatant.

Abbreviations: Glc, cell-specific glucose consumption rate; n.d., not determined; p.i., postinfection; qLac, cell-specific lactate production rate; qNH4+: cell-specific ammonium production rate; qmax., maximum; SF, shake flask; VCC, viable cell concentration.

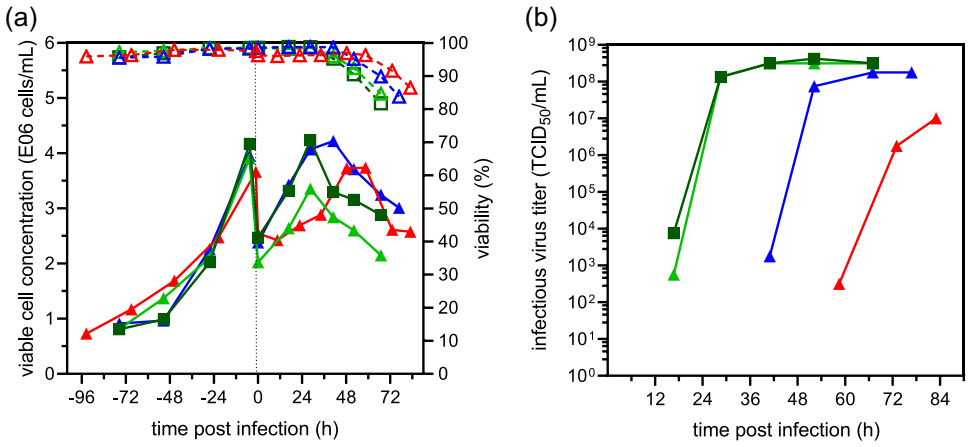


**FIGURE 4** rVSV-NDV production in CCX.E10 cells in 1 L (triangles) and 3 L STRs (squares) in batch mode. All cultures were infected at an MOI of 1E-4 at $2 \times 10^6$ cells/mL following a two-fold dilution step with fresh medium. (a) Viable cell concentration (solid lines, full symbols) and viability (dashed lines, empty symbols) for STRs operated with 80 rpm (red), 130 rpm (blue), 180 rpm (light (1 L STR) + dark green (3 L STR)). (b) Infectious virus titer. CCX.E10, QOR2/2E11 cells; MOI, multiplicity of infection; rVSV-NDV, recombinant hybrid virus: VSV backbone and surface glycoproteins of NDV used in this study; STRs, stirred tank bioreactors.

at 80 rpm resulted in complete consumption of glucose until the TOI (Figure S1A). Over the course of the virus production phase, no limitation in glucose was observed at 80 rpm as well as 180 rpm regardless of the scale (Figure S1C,D). Due to the prolonged growth phase at 130 rpm, glucose was depleted at 48 hpi (Figure S1B). Moreover, as a consequence of cell death and release of intracellular metabolites, ammonium concentrations increased but stayed below 1 mM for all conditions. The highest lactate concentrations were reached at 130 rpm, exceeding 30 mM at 36 hpi (Figure S1B). Variation of agitation speed had no effect on $q_{glc}$ and cell-specific lactate ($q_{lac}$) or ammonium ($q_{NH4}$) release rate (Table 2). However, $q_{glc}$ and $q_{lac}$ were about 2–3 times higher compared with cultivations in shake flasks, which may indicate a higher cell stress (from stirring or aeration) compared with orbitally shaken systems.

Surprisingly, the different stirrer speeds had only a major impact on virus replication. Maximum infectious virus titers of $3.2 \times 10^8$ $TCID_{50}$/mL, $1.8 \times 10^8$ $TCID_{50}$/mL, and $1 \times 10^7$ $TCID_{50}$/mL were reached 36 hpi, 72 hpi, and 84 hpi for 180 rpm, 130 rpm, and 80 rpm, respectively (Figure 4b). Overall, extended cell growth phases after infection were observed for lower agitation speeds. CSVY's of 3 $TCID_{50}$/cell for 80 rpm, 42 $TCID_{50}$/cell for 130 rpm, and 94 $TCID_{50}$/cell for 180 rpm (Table 2) were obtained. Compared with optimized batch runs with BHK-21 cells (the previously identified best producer cell line), slightly lower maximum virus titers (0.3 log) were obtained (Göbel, 2023). However, this is within the standard deviation of our $TCID_{50}$ assay (Genzel, 2014b). Moreover, the highest CSVY obtained in STRs was 20% lower compared to CSVY's obtained in orbitally shaken systems. While high stirring speeds, and consequently increased agitator-dependent shear stress, can result in drastically reduced virus titers for, for example, measles virus (Grein et al., 2019), this was clearly not an issue here. Cell-damaging effects of aeration and bubble bursting have also been identified as another factor influencing cell growth and virus production in STRs (Grein et al., 2019; Chisti, 2000). Michaels et al. (1996). found that low agitation speeds (below 200 rpm) can cause cell-to-bubble interactions leading to increased cell damage. However, due to the low reactor heights and volume flows (3 L/h) in small-scale laboratory processes, this should be negligible. We suspect the limitation of glucose or the accumulation of inhibiting molecules (e.g., lactate) to be the reason for the drastic reduction in viral titers for 80 and 130 rpm. While addition of fresh medium at TOI increased glucose concentrations to 10 mM for 80 rpm, the cells were likely not in an optimal metabolic state at the time of infection. Low glucose levels can lead to metabolic shifts prioritizing cell maintenance over growth and proliferation, as well as a reduction in the levels of phosphorylated precursors required for enzymatic syntheses and draining of intracellular pools of compounds required for protein or membrane synthesis. As a consequence, virus replication could also be impeded compared to cells infected at a late exponential growth phase with a surplus of substrate supply. Furthermore, OVs in particular, are dependent on the host cell glycolysis, and delayed reactivation of host cell glycolysis modulated by rVSV-NDV after infection could further negatively impact virus replication (Goyal & Rajala, 2023). For production at 130 rpm, glucose limitation and the high lactate concentration at 48 hpi, before maximum titers were reached, most likely had a negative impact on virus replication.

Performance of subsequent virus purification trains depends on several factors, that is, the accumulation of protein and host cell DNA in the medium. To assess the potential burden, the impact of process conditions on impurity levels were examined to determine the optimal harvest time point. Following host cell DNA and total protein levels over time, we determined the best time of harvest (maximum infectious virus titer, minimum impurity levels in the supernatant) to be 83 hpi for 80 rpm, 67 hpi for 130 rpm, and 35 hpi for 180 rpm. As cells grew to the highest VCC after infection for 130 rpm, higher host cell DNA concentrations were expected (Table 2). Interestingly, protein concentrations at the optimal harvest time point were around 2-2.5 mg/mL for all conditions. Similar DNA and protein contents in avian AGE1.CR.pIX cell and MDCK-derived STR batch harvests have been described before and efficiently tackled by subsequent purification trains (Gränicher, 2021; Marichal-Gallardo et al., 2017).

In the last step, the process was transferred to a 3 L bioreactor. As the scale-up was carried out within the same order of magnitude, agitation speed (180 rpm) was kept constant. To ensure homogeneous mixing, two pitched-blade impellers were used. Moreover, gas flow rates were scaled proportionally to the increased vw. A comparable cell growth with high viabilities (above 96%) and a $\mu$ of 0.024 1/h was achieved (Figure 4a). By addition of fresh medium at TOI, levels of nutrients were recovered to some extent, and accumulated by-products were diluted. Similar to the 1 L STR operated at 180 rpm, no limitation of glucose was found over the process time (Figure S1D). Even though lactate accumulated rapidly after infection, concentrations remained moderate, increasing, but not exceeding 25 mM in the late infection phase (Figure S1D). rVSV-NDV dynamics, as well as the determined metabolic rates, were very similar to those obtained at the 1 L scale (Figure 4b, Table 2), indicating a successful scale-up. The maximum infectious virus titer was $4.2 \times 10^8$ $TCID_{50}$/mL, corresponding to a CSVY of 100 $TCID_{50}$/cell. Host cell DNA (14.1 µg/mL dsDNA) and total protein (2.0 mg/mL total) impurity levels in the supernatant were also in line with results obtained at the 1 L scale (Table 2). While a transfer to 3 L STR does not constitute a significant scale-up, the similar performance by implementation of two pitched-blade impellers sets the first benchmark for further increase in production volumes. The finding that similar virus titers and productivities were also achieved, indicates the usefulness of both bioreactor systems for efficient rVSV-NDV production. Currently, virus production under cGMP conditions of most manufacturers relies on stainless steel STRs but also on single-use vessels (Zhou et al., 2010). However, orbitally shaken bioreactors also fulfill these requirements without the need of stirrers, which introduce additional shear stress and raise costs in single-use applications. Further experiments are necessary to better understand how the choice of the bioreactor system will impact optimized virus production, e.g. at high cell density and potential formation of syncytia. Adjustments in medium formulation at TOI as demonstrated for BHK-21 and HEK293 cells, could further improve virus titers in batch mode (Göbel, 2023). Furthermore, higher yields could be potentially obtained in perfusion mode with retention devices that enable continuous virus harvesting and reduce virus degradation (Göbel, 2023; Gränicher, 2021).

### 3.4 | Cultivation in ambr15: Scale down and pH evaluation

In a final step, the production process was scaled down to an ambr15 system. Here, the traditional scale-up rule of "equal tip speed" was used for scale-down, rather than the "power per unit volume" approach (Amanullah et al., 2003; Nienow, 2021; Nienow et al., 2013; Tajsoleiman et al., 2019). To evaluate if cell growth and virus

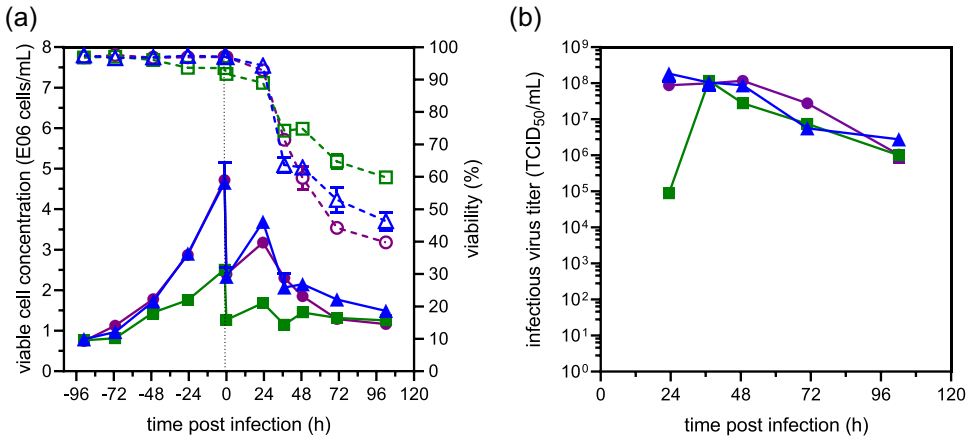


**FIGURE 5** Effect of pH on cell growth (a) and rVSV-NDV production (b) in CCX.E10 cells in 15 mL ambr15 STR vessels in batch mode. Ambr15 vessels were inoculated at $0.8 \times 10^6$ cells/mL and operated in batch mode at the respective pH set point. At time of infection a two-fold dilution with fresh medium containing virus (MOI: 1E-4) was carried out. (a) Viable cell concentration (solid lines, full symbols) and viability (dashed lines, empty symbols) for STRs operated at pH 7.0 (green squares), pH 7.2 (blue triangles), and pH 7.4 (purple circles). (b) Infectious virus titer. Values are reported as the mean ± SD of a duplicate with two independent ambr15 vessels. CCX.E10, QOR2/2E11 cells; MOI, multiplicity of infection; rVSV-NDV, recombinant hybrid virus: VSV backbone and surface glycoproteins of NDV used in this study; SD, standard deviation; STRs, stirred tank bioreactors.

production could be further improved, different pH values ranging from 7.0 to 7.4 were tested. As expected, pH had a strong impact on cell growth (Figure 5a). While cell growth was already severely impeded at pH 7.0, there was no difference for pH 7.2 and 7.4. Maximum cell-specific growth rates of 0.020–0.022 1/h were achieved, comparable to growth rates achieved at the 1 and 3 L scale STR (Table 2). After infection, a steep decline in cell viability was noticeable starting from 24 hpi (Figure 5a). While a reduction of temperature to 34°C had no positive effect on virus production for rVSV-NDV, drastic declines in cell viability were prevented in STRs for both CCX.E10 and BHK-21 cells (Göbel, 2023; Figure 4a). Despite the impeded cell growth at pH 7.0, maximum infectious virus titers of $1.0–2.0 \times 10^8$ $TCID_{50}$/mL were achieved for all conditions respectively. This resulted in decreasing CSVYs (70, 59, and 36 $TCID_{50}$/cell) for increasing pH values (7.0, 7.2, and 7.4). While there was no measurable difference in terms of maximum titer, pH 7.0 resulted in a delayed virus replication, achieving maximum titers at 36 hpi compared with 24 hpi for pH 7.2 and 7.4 (Figure 5b). Stability of virions can be affected by absorption to cellular debris and release of cellular proteases after virus-induced apoptosis and cell lysis, therefore, lower stability was expected in the ambr15 system from 24 hpi compared with STRs or orbitally shaken systems. Moreover, low pH values (below 7.0) are generally found to negatively impact virus production and stability (Ferreira et al., 2007; Zimmer et al., 2013). For the tested pH range, however, stability was not impacted. Due to the impeded cell growth at pH 7.0, a biphasic process could be designed, controlling the pH between 7.2 and 7.4 for the cell growth phase and lowering the pH set-point to 7.0 after infection to minimize cell growth and thereby reduce the level of contaminants, to facilitate the design of subsequent clarification trains and further process intensification strategies. Nevertheless, the ambr15 system was identified as a suitable small scale system for process optimization, reaching similar cell growth parameters and virus titers as compared with larger scale STRs.

## 4 | CONCLUSION

In this study, CCX.E10 cells were identified as a viable host cell substrate for the manufacturing of the fusogenic oncolytic virus, rVSV-NDV. CCX.E10 cells demonstrated robust growth to high concentrations in batch mode with low accumulation rates of metabolic by-products such as lactate and ammonium. Moreover, they could be cultivated in various systems, including shake flasks, OSB, STR and ambr15 with similar cell growth performance and high virus yields.

Maximum infectious virus titers above $10^8$ $TCID_{50}$/mL with high CSVYs were reached regardless of the bioreactor system selected. Compared to other suspension cells infected in optimized batch STR processes, similar (BHK-21 cells) or drastically higher (HEK293 and AGE1.CR cells) volumetric virus productivities were achieved with CCX.E10 (Göbel, 2023). While oncolytic applications could possibly allow the use of production cell lines known to be tumorigenic (e.g., BHK-21 cells) due to the unique risk–benefit ratio compared with other (i.e., prophylactic) applications, regulatory authorities would likely require additional purity and safety studies to demonstrate a satisfactory quality profile, which introduces additional cost, time, and risk to the process. Therefore, the identification of a cell line that produces high yields of virus product, while also offering a de-risked regulatory pathway, represents a valuable step in process development.

With regard to downstream processing, harvesting at the time-point of maximum virus titer resulted in maximum dsDNA concentrations of 14.1 µg/mL and protein contamination of 2.0 mg/mL at the 3 L STR (180 rpm), respectively. Chromatography-based purification methods including steric exclusion chromatography have been

reported to allow effective handling of such impurity levels (Marichal-Gallardo et al., 2017). Additional screening and testing of the produced OV regarding oncolytic potency, efficacy in preclinical models as well as whole blood and serum stability in human and animal systems should be carried out. Current OV platforms require a dose input of $10^9$–$10^{10}$ virions/injection to achieve a therapeutic effect and effective delivery to tumor sites. Therefore, development of OV production processes that allow to generate even higher virus yields is essential. Process intensification by transition from batch production to perfusion mode could further increase titers as much higher cell concentrations can be reached (Genzel et al., 2014a; Göbel, 2023; Gränicher, 2021; Nikolay et al., 2018; Lavado-García et al., 2020; Wu et al., 2021).

Taken together, the CCX.E10 cell line is a promising host for industrial production of OVs due to the high cell concentrations obtained in the chemically-defined medium in batch mode and options for scale-up. The ability to achieve similarly high rVSV-NDV yields, regardless of the production system used, as well as compliance of the cell line with regulatory guidelines, makes it an attractive host for large-scale production of this virus and potentially other similar fusogenic viruses that are under development as clinical oncolytic viral drug products.

## AUTHOR CONTRIBUTIONS

*Conceptualization*: Sven Göbel, Karim E. Jaén, Rita P. Fernandes, Yvonne Genzel, Udo Reichl, and Jennifer Altomonte. *Methodology*: Sven Göbel, Karim E. Jaén, Rita P. Fernandes, and Yvonne Genzel. *Investigation*: Sven Göbel and Karim E. Jaén. *Writing—original draft*: Sven Göbel. *Writing—review and editing*: Sven Göbel, Karim E. Jaén, Rita P. Fernandes, Manfred Reiter, Udo Reichl, Jennifer Altomonte, and Yvonne Genzel. *Supervision*: Yvonne Genzel, Udo Reichl, and Jennifer Altomonte. *Project administration*: Sven Göbel, Karim E. Jaén, and Yvonne Genzel.

## ACKNOWLEDGMENTS

The authors would like to thank Corina Siewert for the excellent technical support regarding general lab work and cell culture. The authors would like to thank Carole Langlois and Diogo Mattos from Sartorius for allowing us to use their ambr15 for these experiments. Furthermore, the kind support from Kühner (Tibor Anderlei) with discussions for the OSB10 run, ProBioGen for providing the adherent AGE1.CR.pIX cells, and Marc Hein for carrying out initial experiments are equally acknowledged, Part of the funding for this work was provided by the EXIST-Forschungstranfser Program (financed by the Federal Ministry for Economic Affairs and Energy) under the grant agreement #03EFOBY215 awarded to J. Altomonte.

## CONFLICT OF INTEREST STATEMENT

J. Altomonte (WO 2017/198779) holds a patent for the development and use of rVSV-NDV for oncolytic therapy of cancer and is cofounder of Fusix Biotech GmbH, which is developing the rVSV-NDV technology for clinical use. M. Reiter is an employee of Nuvonis Technologies, which owns the CCX.E10 cells.

## DATA AVAILABILITY STATEMENT

The data that support the findings of this study are available from the corresponding author upon reasonable request. Data is available in article's supplementary material. Additional data is available on request from the authors. The data that support the findings of this study are available from the corresponding author, Yvonne Genzel, upon reasonable request.

## ETHICS STATEMENT

This article does not contain any studies with human participants or animals performed by any of the authors.

## ORCID

*Sven Göbel* http://orcid.org/0000-0002-2264-5569

## REFERENCES

Abaandou, L., Quan, D., & Shiloach, J. (2021). Affecting HEK293 cell growth and production performance by modifying the expression of specific genes. *Cells*, *10*(7), 1667.

Abdullahi, S., Jäkel, M., Behrend, S. J., Steiger, K., Topping, G., Krabbe, T., Colombo, A., Sandig, V., Schiergens, T. S., Thasler, W. E., Werner, J., Lichtenthaler, S. F., Schmid, R. M., Ebert, O., & Altomonte, J. (2018). A novel chimeric oncolytic virus vector for improved safety and efficacy as a platform for the treatment of hepatocellular carcinoma. *Journal of Virology*, *92*(23), e01386-18.

Adolf Kühner AG. (2017). User Manual OrbShake Bioreactor SB10-X (# 52409 version 2).

Amanullah, A., Buckland, B. C., & Nienow, A. W. (2003). Mixing in the fermentation and cell culture industries, *Handbook of industrial mixing* (pp. 1071–1170). Wiley & Sons.

Bissinger, T., Fritsch, J., Mihut, A., Wu, Y., Liu, X., Genzel, Y., Tan, W. S., & Reichl, U. (2019). Semi-perfusion cultures of suspension MDCK cells enable high cell concentrations and efficient influenza A virus production. *Vaccine*, *37*(47), 7003–7010.

Chisti, Y. (2000). Animal-cell damage in sparged bioreactors. *Trends in Biotechnology*, *18*(10), 420–432.

Coronel, J., Behrendt, I., Bürgin, T., Anderlei, T., Sandig, V., Reichl, U., & Genzel, Y. (2019). Influenza A virus production in a single-use orbital shaken bioreactor with ATF or TFF perfusion systems. *Vaccine*, *37*(47), 7011–7018.

Coronel, J., Gränicher, G., Sandig, V., Noll, T., Genzel, Y., & Reichl, U. (2020). Application of an inclined settler for cell culture-based influenza A virus production in perfusion mode. *Frontiers in Bioengineering and Biotechnology*, *8*, 672–673.

Elahi, S. M., Shen, C. F., & Gilbert, R. (2019). Optimization of production of vesicular stomatitis virus (VSV) in suspension serum-free culture medium at high cell density. *Journal of Biotechnology*, *289*, 144–149.

EMA. (2015). Assessment report Imlygic. Committee for Medicinal Products for Human Use (CHMP).

Ferreira, T. B., Carrondo, M. J. T., & Alves, P. M. (2007). Effect of ammonia production on intracellular pH: Consequent effect on adenovirus vector production. *Journal of Biotechnology*, *129*(3), 433–438.

Flint, S. J., Racaniello, V. R., Rall, G. F., Hatziioannou, T., & Skalka, A. M. (2020). *Principles of virology: Pathogenesis and control* (Vol. 2). John Wiley & Sons.

Genzel, Y., Rödig, J., Rapp, E., & Reichl, U. (2014). Vaccine production: Ustream processing with adherent or suspension cell Lines. *Animal Cell Biotechnology: Methods and Protocols*, *1104*, 371–393.

Genzel, Y., Vogel, T., Buck, J., Behrendt, I., Ramirez, D. V., Schiedner, G., Jordan, I., & Reichl, U. (2014a). High cell density cultivations by

alternating tangential flow (ATF) perfusion for influenza A virus production using suspension cells. *Vaccine*, *32*(24), 2770–2781.

Giese, H., Klöckner, W., Peña, C., Galindo, E., Lotter, S., Wetzel, K., Meissner, L., Peter, C. P., & Büchs, J. (2014). Effective shear rates in shake flasks. *Chemical Engineering Science*, *118*, 102–113.

Göbel, S., Jaén, K. E., Dorn, M., Neumeyer, V., Jordan, I., Sandig, V., Reichl, U., Altomonte, J., & Genzel, Y. (2023). Process intensification strategies towards cell culture-based high-yield production of a fusogenic oncolytic virus. *Biotechnology and Bioengineering*. Advance online publication.

Göbel, S., Kortum, F., Chavez, K. J., Jordan, I., Sandig, V., Reichl, U., Altomonte, J., & Genzel, Y. (2022). Cell-line screening and process development for a fusogenic oncolytic virus in small-scale suspension cultures. *Applied Microbiology and Biotechnology*, *106*(13–16), 4945–4961.

González Hernández, Y. (2007). Serum-free culturing of mammalian cells–adaptation to and cryopreservation in fully defined media. *ALTEX: Alternativen zu Tierexperimenten*, *24*(2), 110–116.

Goyal, P., & Rajala, M. S. (2023). Reprogramming of glucose metabolism in virus infected cells. *Molecular and Cellular Biochemistry*. Advance online publication.

Gränicher, G., Babakhani, M., Göbel, S., Jordan, I., Marichal-Gallardo, P., Genzel, Y., & Reichl, U. (2021). A high cell density perfusion process for modified vaccinia virus Ankara production: process integration with inline DNA digestion and cost analysis. *Biotechnology and Bioengineering*, *118*(12), 4720–4734.

Gränicher, G., Coronel, J., Pralow, A., Marichal-Gallardo, P., Wolff, M., Rapp, E., Karlas, A., Sandig, V., Genzel, Y., & Reichl, U. (2019). Efficient influenza A virus production in high cell density using the novel porcine suspension cell line PBG.PK2.1. *Vaccine*, *37*(47), 7019–7028.

Gränicher, G., Coronel, J., Trampler, F., Jordan, I., Genzel, Y., & Reichl, U. (2020). Performance of an acoustic settler versus a hollow fiber–based ATF technology for influenza virus production in perfusion. *Applied Microbiology and Biotechnology*, *104*(11), 4877–4888.

Grein, T. A., Loewe, D., Dieken, H., Weidner, T., Salzig, D., & Czermak, P. (2019). Aeration and shear stress are critical process parameters for the production of oncolytic measles virus. *Frontiers in Bioengineering and Biotechnology*, *7*(78), fbioe.2019.00078.

Hesterberg, R., Cleveland, J., & Epling-Burnette, P. (2018). Role of polyamines in immune cell functions. *Medical Sciences*, *6*(1), 22.

ICH. (1998). Quality of biotechnological products: Derivation and characterisation of cell substrates used for production of biotechnological/biological products. ICH harmonised tripartite guideline. *Developments in Biological Standardization*, *93*, 223–234.

Jordan, I., & Sandig, V. (2014). Matrix and backstage: Cellular substrates for viral vaccines. *Viruses*, *6*(4), 1672–1700.

Klöckner, W., Diederichs, S., & Büchs, J. (2014). Orbitally shaken single-use bioreactors. *Advances in Biochemical Engineering/Biotechnology*, *138*, 45–60.

Krabbe, T., Marek, J., Groll, T., Steiger, K., Schmid, R. M., Krackhardt, A. M., & Altomonte, J. (2021). Adoptive T cell therapy is complemented by oncolytic virotherapy with fusogenic VSV-NDV in combination treatment of murine melanoma. *Cancers*, *13*(5), 1044.

Kraus, B., von Fircks, S., Feigl, S., Koch, S. M., Fleischanderl, D., Terler, K., Dersch-Pourmojib, M., Konetschny, C., Grillberger, L., & Reiter, M. (2011). Avian cell line - Technology for large scale vaccine production. *BMC Proceedings*, *5*(Suppl. 8), P52.

Lavado-García, J., Cervera, L., & Gòdia, F. (2020). An alternative perfusion approach for the intensification of virus-like particle production in HEK293 cultures. *Frontiers in Bioengineering and Biotechnology*, *8*, 617.

Lohr, V. (2014). Characterization of the avian designer cells AGE1.CR and AGE1.CR.pIX considering growth, metabolism and production of influenza virus and modified vaccinia virus Ankara (MVA) bioprocess engineering, *Max Planck Institute for Dynamics of Complex Technical Systems*, Otto-von-Guericke Universität, Magdeburg. https://hdl.handle.net/11858/00-001M-0000-0024-3EDE-2

Lohr, V., Hädicke, O., Genzel, Y., Jordan, I., Büntemeyer, H., Klamt, S., & Reichl, U. (2014). The avian cell line AGE1.CR.pIX characterized by metabolic flux analysis. *BMC Biotechnology*, *14*(1), 72.

Marichal-Gallardo, P., Pieler, M. M., Wolff, M. W., & Reichl, U. (2017). Steric exclusion chromatography for purification of cell culture-derived influenza A virus using regenerated cellulose membranes and polyethylene glycol. *Journal of Chromatography A*, *1483*, 110–119.

Meier, K., Klöckner, W., Bonhage, B., Antonov, E., Regestein, L., & Büchs, J. (2016). Correlation for the maximum oxygen transfer capacity in shake flasks for a wide range of operating conditions and for different culture media. *Biochemical Engineering Journal*, *109*, 228–235.

Michaels, J. D., Mallik, A. K., & Papoutsakis, E. T. (1996). Sparging and agitation-induced injury of cultured animals cells: Do cell-to-bubble interactions in the bulk liquid injure cells? *Biotechnology and Bioengineering*, *51*(4), 399–409.

Newsholme, P., Procopio, J., Lima, M. M. R., Pithon-Curi, T. C., & Curi, R. (2003). Glutamine and glutamate—Their central role in cell metabolism and function. *Cell Biochemistry and Function*, *21*(1), 1–9.

Nienow, A. W. (2021). The impact of fluid dynamic stress in stirred bioreactors–the scale of the biological entity: A personal view. *Chemie Ingenieur Technik*, *93*(1–2), 17–30.

Nienow, A. W., Rielly, C. D., Brosnan, K., Bargh, N., Lee, K., Coopman, K., & Hewitt, C. J. (2013). The physical characterisation of a microscale parallel bioreactor platform with an industrial CHO cell line expressing an IgG4. *Biochemical Engineering Journal*, *76*, 25–36.

Nikolay, A., Léon, A., Schwamborn, K., Genzel, Y., & Reichl, U. (2018). Process intensification of EB66® cell cultivations leads to high-yield yellow fever and Zika virus production. *Applied Microbiology and Biotechnology*, *102*(20), 8725–8737.

Petiot, E., Cuperlovic-Culf, M., Shen, C. F., & Kamen, A. (2015). Influence of HEK293 metabolism on the production of viral vectors and vaccine. *Vaccine*, *33*(44), 5974–5981.

Petiot, E., Proust, A., Traversier, A., Durous, L., Dappozze, F., Gras, M., Guillard, C., Balloul, J. M., & Rosa-Calatrava, M. (2018). Influenza viruses production: Evaluation of a novel avian cell line DuckCelt®-T17. *Vaccine*, *36*(22), 3101–3111.

Reiter, M., Portsmouth, D., & Barrett, P. N. (2014). Avian suspension culture cell lines for production of vaccines and other biologicals, *Industrial scale suspension culture of living cells* (pp. 390–409). Wiley & Sons.

Schiefelbein, S., Fröhlich, A., John, G. T., Beutler, F., Wittmann, C., & Becker, J. (2013). Oxygen supply in disposable shake-flasks: prediction of oxygen transfer rate, oxygen saturation and maximum cell concentration during aerobic growth. *Biotechnology Letters*, *35*(8), 1223–1230.

Schneider, M. (1996). The importance of ammonia in mammalian cell culture. *Journal of Biotechnology*, *46*(3), 161–185.

Tajsoleiman, T., Mears, L., Krühne, U., Gernaey, K. V., & Cornelissen, S. (2019). An industrial perspective on scale-down challenges using miniaturized bioreactors. *Trends in Biotechnology*, *37*(7), 697–706.

Tan, R.-K., Eberhard, W., & Büchs, J. (2011). Measurement and characterization of mixing time in shake flasks. *Chemical Engineering Science*, *66*(3), 440–447.

Tsao, Y.-S., Cardoso, A. G., Condon, R. G. G., Voloch, M., Lio, P., Lagos, J. C., Kearns, B. G., & Liu, Z. (2005). Monitoring Chinese hamster ovary cell culture by the analysis of glucose and lactate metabolism. *Journal of Biotechnology*, *118*(3), 316–327.

Ungerechts, G., Bossow, S., Leuchs, B., Holm, P. S., Rommelaere, J., Coffey, M., Coffin, R., Bell, J., & Nettelbeck, D. M. (2016). Moving oncolytic viruses into the clinic: Clinical-grade production,

purification, and characterization of diverse oncolytic viruses. *Molecular Therapy: Methods & Clinical Development*, *3*, 16018.

Vázquez-Ramírez, D., Genzel, Y., Jordan, I., Sandig, V., & Reichl, U. (2018). High-cell-density cultivations to increase MVA virus production. *Vaccine*, *36*(22), 3124–3133.

Wu, Y., Bissinger, T., Genzel, Y., Liu, X., Reichl, U., & Tan, W. S. (2021). High cell density perfusion process for high yield of influenza A virus production using MDCK suspension cells. *Applied Microbiology and Biotechnology*, *105*(4), 1421–1434.

Wurm, M. J., & Wurm, F. M. (2021). Naming CHO cells for bio-manufacturing: Genome plasticity and variant phenotypes of cell populations in bioreactors question the relevance of old names. *Biotechnology Journal*, *16*(7), 2100165.

Zdrojewicz, Z., & Lachowski, M. (2014). The importance of putrescine in the human body. *Postępy Higieny i Medycyny Doświadczalnej*, *68*, 393–403.

Zhou, W., Seth, G., Guardia, M. J., & Hu, W.-S. (2010). Mammalian cell bioreactors. *Encyclopedia of Industrial Biotechnology*, *1*, 1–10.

Zimmer, B., Summermatter, K., & Zimmer, G. (2013). Stability and inactivation of vesicular stomatitis virus, a prototype rhabdovirus. *Veterinary Microbiology*, *162*(1), 78–84.

## SUPPORTING INFORMATION

Additional supporting information can be found online in the Supporting Information section at the end of this article.

**How to cite this article:** Göbel, S., Jaén, K. E., Fernandes, R. P., Reiter, M., Altomonte, J., Reichl, U., & Genzel, Y. (2023). Characterization of a quail suspension cell line for production of a fusogenic oncolytic virus. *Biotechnology and Bioengineering*, *120*, 3335–3346. https://doi.org/10.1002/bit.28530